Control of high-energy high-power densities storage devices by Li-ion battery and supercapacitor for fuel cell/photovoltaic hybrid power plant for autonomous system applications

Sikkabut, Suwat; Mungporn, Pongsiri; Ekkaravarodome, Chainarin; Bizon, Nicu; Tricoli, Pietro; Nahid-Mobarakeh, Babak; Pierfederici, Serge; Davat, Bernard; Thounthong, Phatiphat

DOI:
10.1109/TIA.2016.2581138

Control of High-Energy High-Power Densities Storage Devices by Li-ion Battery and Supercapacitor for Fuel Cell/Photovoltaic Hybrid Power Plant for Autonomous System Applications

Suwat Sikkabut, Pongsiri Mungporn, Chainarin Ekkaravarodome, *Member*, *IEEE*, Nicu Bizon, *Member, IEEE,* Pietro Tricoli, *Member, IEEE,* Babak Nahid-Mobarakeh, *Senior Member, IEEE*, Serge Pierfederici, Bernard Davat, *Member, IEEE,* and Phatiphat Thounthong, *Senior Member, IEEE*

Abstract—**This study presents an energy management approach for a hybrid energy system comprised of a photovoltaic (PV) array and a polymer electrolyte membrane fuel cell (PEMFC). Two storage devices (a Li-ion battery module and a supercapacitor (SC) bank) are used in the proposed structure as a high-energy high-power density storage device. Multi-segment converters for the PV, FC, battery, and SC are proposed for grid independent applications. Nonlinear differential flatness-based fuzzy logic control for dc bus voltage stabilization for power plant are investigated. To validate the control approach, a hardware system is realized with analog circuits for the PV, FC, battery, and SC current control loops (inner controller loops) and with numerical calculation (dSPACE) for the external energy control loop. Experimental results with small-scale devices [a photovoltaic array (800 W, 31 A), a PEMFC (1200 W, 46 A), a Li-ion battery module (11.6 Ah, 24 V), and a SC bank (100 F, 32 V)] demonstrate the excellent energy-management scheme during load cycles.**

Index Terms-- **Flatness control, fuel cells (FCs), fuzzy logic, Li-Ion battery, nonlinear system, photovoltaic (PV), supercapacitor (SC).**

I. Introduction

Solar power source is one of the most promising renewable power generation technology [1], [2]. FCs also show great potential to be green power sources of the near future because of many advances they have (such as low emission of pollutant gases, high efficiency, and flexible modular structure) [3]. However, each source has its own drawbacks. For instance, solar power is highly dependent on climate while FCs need hydrogen-rich fuel. FCs are good energy sources to provide reliable power at a steady rate, but they cannot respond to the electrical load transients as fast as desired. This is mainly due to their slow internal electrochemical and thermodynamic responses [4], [5], [6].

Because different alternative energy sources can complement each other, the multisource hybrid alternative energy systems (with proper control) have great potential to provide higher quality and more reliable power to customers than a system based on a single resource. Moreover, to overcome the PV and FC drawbacks, the system can be combined with other energy storage devices with fast dynamics, such as battery or SC, to form a hybrid power generation system [7], [8].

The specific energy of batteries is usually high, but the specific power is relatively low. On the other hand, the specific energy stored in an SC is comparatively lower, but the specific power is rather large due to the short time constant of double layer charging [9], [10]. Therefore, a combination of both devices in a hybrid system appears to be reasonable: the high energy content of the battery and the high power of the SC [11], [12].

In this paper, a hybrid alternative energy system consisting

This work was supported in part by the research program in cooperation with the Faculty of Technical Education and Thai-French Innovation Institute (TFII), King Mongkut's University of Technology North Bangkok (KMUTNB) with Université de Lorraine (UL), and in part by the Thailand Research Fund and (Research Grant for Mid-Career University Faculty) under Grant RSA5580009 and KMUTNB-GOV-59-12.

S. Sikkabut and P. Mungporn are with the Renewable Energy Research Centre (RERC), Thai-French Innovation Institute, King Mongkut's University of Technology North Bangkok, Bangkok 10800, Thailand (e-mail: suwatsi@kmutnb.ac.th , pongsirim@kmutnb.ac.th).

C. Ekkaravarodome is with the Department of Instrumentation and Electronics Engineering, Faculty of Engineering, King Mongkut's University of Technology North Bangkok, Bangkok 10800, Thailand (e-mail: chainarine@kmutnb.ac.th).

N. Bizon is with the Faculty of Electronics, Communication and Computers University of Pitesti, 110040 Pitesti, 1 Targu din Vale, Arges county, Romania (e-mail: nicubizon@yahoo.com , nicu.bizon@upit.ro).

P. Tricoli is with the Department of Electronic, Electrical and Systems Engineering, University of Birmingham, Birmingham B15 2TT, UK (e-mail: p.tricoli@bham.ac.uk).

B. Nahid-Mobarakeh, S. Pierfederici, and B. Davat are with the Groupe de Recherche en Electrotechnique et Electronique de Nancy (GREEN), Université de Lorraine, Nancy-Lorraine, France (e-mail: babak.Nahidmobarakeh@univ-lorraine.fr, Serge.Pierfederici@univ-lorraine.fr, Bernard.Davat@ensem.inpl-nancy.fr).

P. Thounthong is with the Renewable Energy Research Centre (RERC), Department of Teacher Training in Electrical Engineering, Faculty of Technical Education, King Mongkut's University of Technology North Bangkok, Bangkok 10800, Thailand (e-mail: phtt@kmutnb.ac.th).

Color versions of one or more of the figures in this paper are available online at http://ieeexplore.ieee.org.

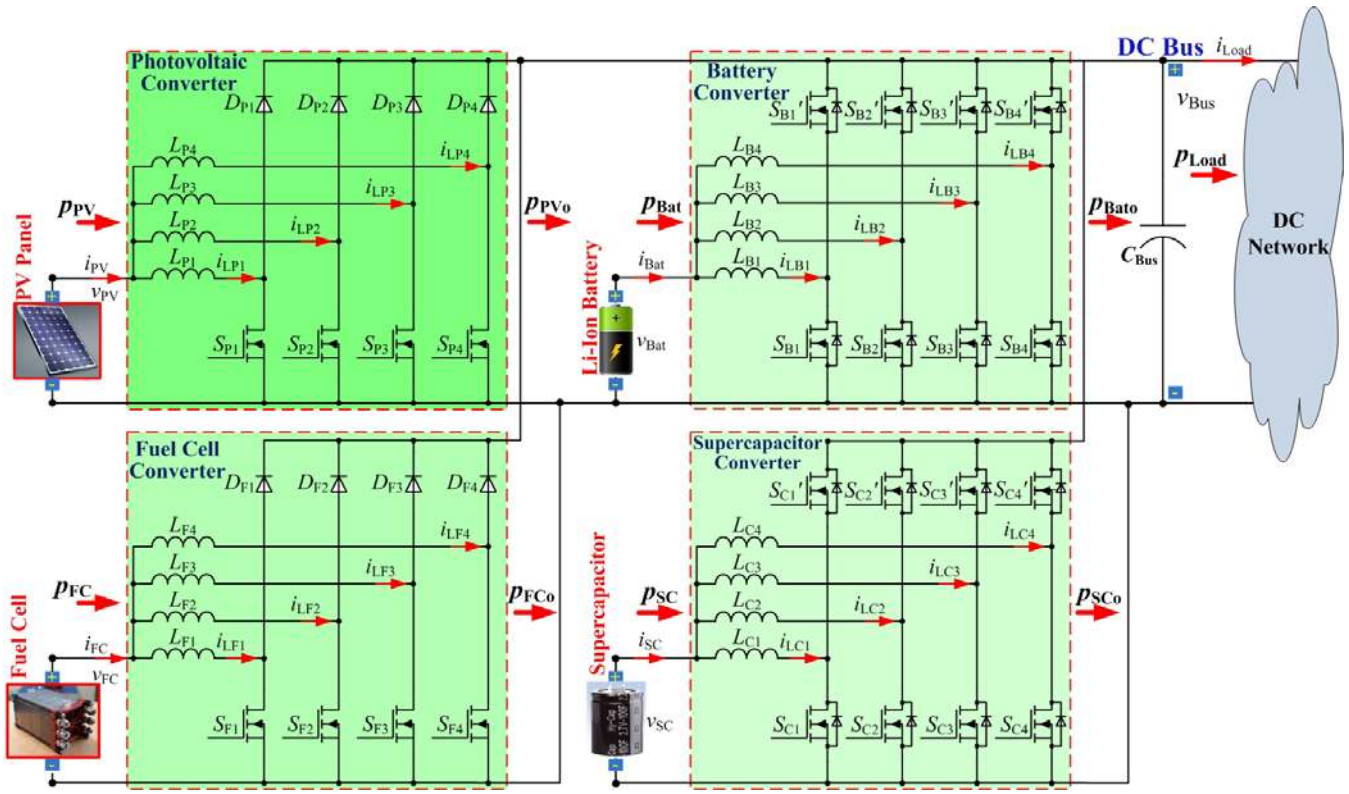

Fig. 1. Proposed power converter structure of a power plant supplied by a PV, an FC with a Li-Ion battery and supercapacitor storage devices, where p_{PV} (= v_{PV}·i_{PV}), v_{PV} and i_{PV} are the PV power, voltage, and current, respectively; p_{FC} (= v_{FC}· i_{FC}), v_{FC} and i_{FC} are the FC power, voltage, and current, respectively; p_{Bat} (= v_{Bat}· i_{Bat}), v_{Bat} and i_{Bat} are the battery power, voltage, and current, respectively; p_{SC} (= v_{SC}· i_{SC}), v_{SC} and i_{SC} are the SC power, voltage, and current, respectively; p_{Load} (= v_{Bus}· i_{Load}), v_{Bus} and i_{Load} are the load power, dc bus voltage, and load current, respectively. P_{PVo}, p_{FCo}, p_{Bato}, and p_{SCo} are the output powers to the dc link from the converters of PV, FC, battery, and supercapacitor, respectively.

of PV, FC, Li-Ion battery and SC is proposed. An intelligent-control (T–S fuzzy logic) law based on a differential flatness estimate of the system is proposed for the dc bus voltage stabilization. The remainder of the paper is structured as follows: the section II details the hybrid energy system and the power plant model. In section III, a proof of the flat system consisting of the hybrid energy power plant, the fuzzy logic control law for dc bus voltage stabilization, the SC, and the battery charging strategies are presented. In section IV, the test bench results for the proposed system are presented. Finally, this paper ends with concluding remarks for further study in section V.

II. Hybrid Power Plant

A. System Configuration Studied

The power converter circuits of the proposed renewable hybrid power plant is presented in Fig. 1. The SC and battery converters has four-phase parallel bidirectional converters (two-quadrant converters) and the FC and PV converters have four-phase parallel boost converters. With interleaved switching technique operation, the current ripple is smaller, consequently, it is achievable to use smaller inductors and capacitors at the input and output of the converter [13], [14], [15]. In addition, interleaved boost converters can also reduce input current ripple and the switching losses, so the efficiency of the converter is improved [16], [17], [18]

For reasons of safety and dynamics, the PV, FC, SC, and battery converters are generally regulated principally by inner current-regulation loops (or power-control loops) based on the classical cascade control structure [5]. The dynamics of inner-control loops are much faster than those of outer control loops, which are described shortly. Consequently, the SC current i_{SC}, the PV current i_{PV}, the FC current i_{FC} and the battery current i_{Bat} are estimated to track completely their set-points of i_{SCREF}, i_{PVREF}, i_{FCREF}, and i_{BatREF}, respectively.

For clarity, the oscilloscope waveforms in Figs. 2 and 3 portray the steady-state characteristics of the proposed interleaved converters for the FC and SC devices at different current set-points. The real test bench was implemented in the laboratory (refer to Appendix).

Fig. 2 illustrates the dc bus voltage, the FC voltage, the FC current, the first, second, third, and forth inductor currents at i_{FCREF} = 44 A; and Fig. 3 portrays the dc bus voltage, the SC voltage, the SC current, the first, second, third, and forth inductor currents at i_{SCREF} = −20 A (charging). One can observe that the source current (total input) is the sum of the inductor currents and that the source ripple current is 1/*N* the individual inductor ripple currents. So, the source ripple current of the four-cell interleaved converter is nearly zero. It means that each source mean current is close to the source rms current at the switching frequency of 25 kHz.

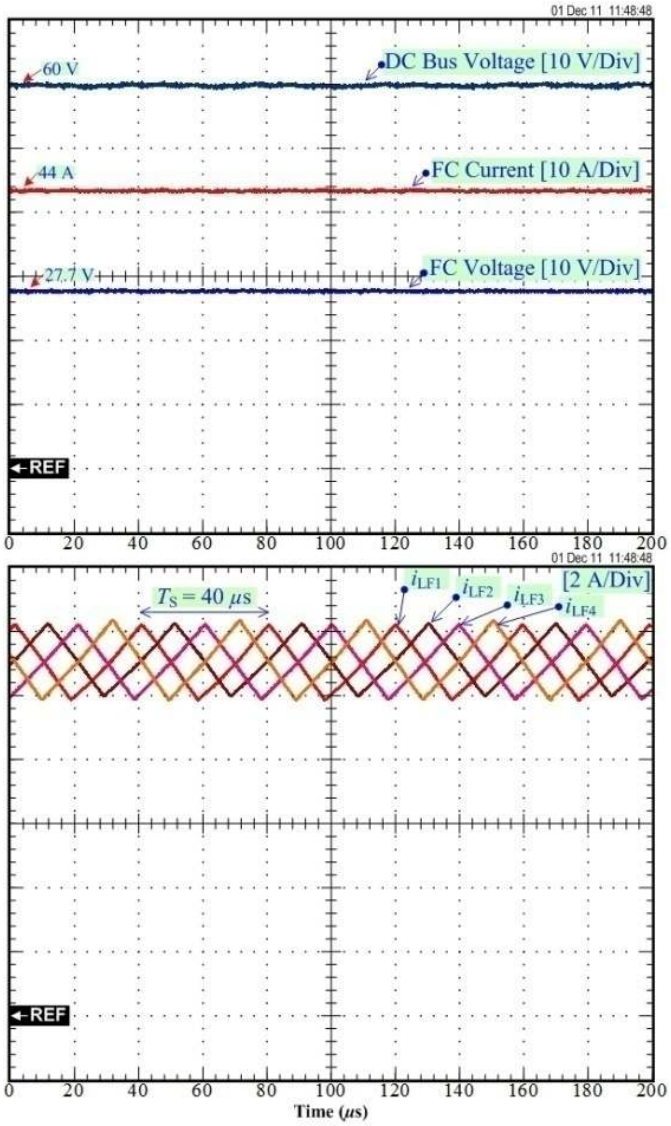

Fig. 2. Steady-state waveforms of the proposed four-cell interleaved FC converter system at an FC current command of 44 A (rated current).

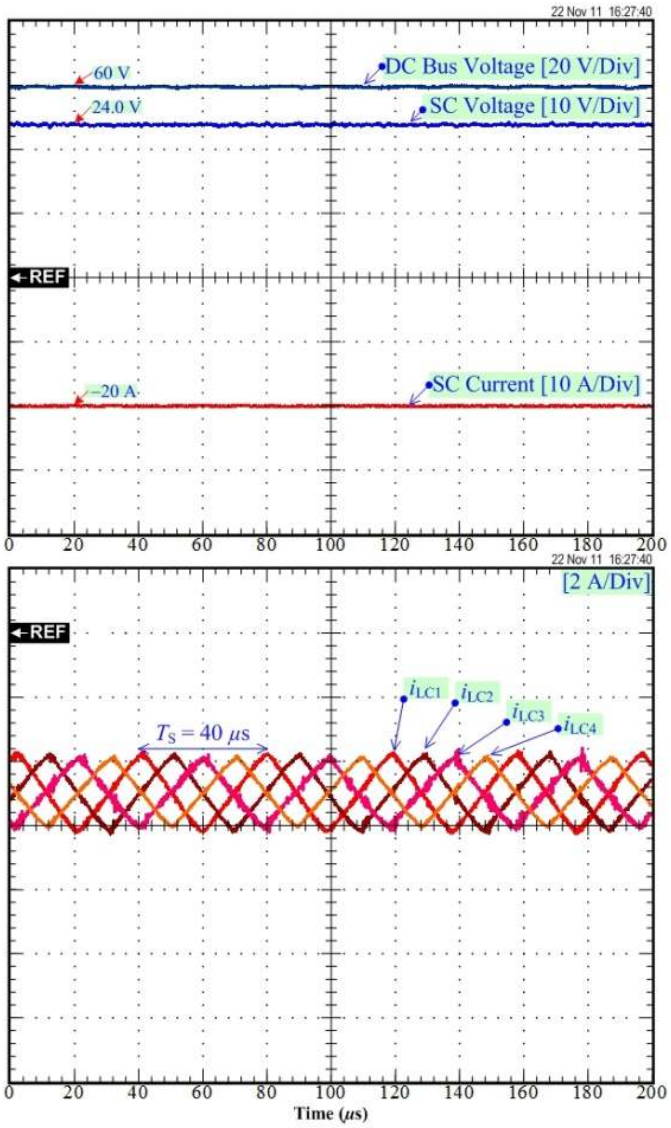

Fig. 3. Steady-state waveforms of the proposed four-cell interleaved SC converter system at a SC current command of −20 A (charging).

B. Model of the Power Plant

The inner control loops of the PV, FC, battery, and SC powers can be estimated as a unity gain. The PV power set-point p_{PVREF}, the FC power set-point p_{FCREF}, the battery power set-point p_{BatREF}, and the SC power set-point p_{SCREF} are

$$p_{\mathrm{PVREF}} = p_{\mathrm{PV}} = v_{\mathrm{PV}} \cdot i_{\mathrm{PVREF}} = v_{\mathrm{PV}} \cdot i_{\mathrm{PV}} \quad (1)$$

$$p_{\mathrm{FCREF}} = p_{\mathrm{FC}} = v_{\mathrm{FC}} \cdot i_{\mathrm{FCREF}} = v_{\mathrm{FC}} \cdot i_{\mathrm{FC}} \quad (2)$$

$$p_{\mathrm{BatREF}} = p_{\mathrm{Bat}} = v_{\mathrm{Bat}} \cdot i_{\mathrm{BatREF}} = v_{\mathrm{Bat}} \cdot i_{\mathrm{Bat}} \cdot \quad (3)$$

$$p_{\mathrm{SCREF}} = p_{\mathrm{SC}} = v_{\mathrm{SC}} \cdot i_{\mathrm{SCREF}} = v_{\mathrm{SC}} \cdot i_{\mathrm{SC}} \cdot \quad (4)$$

Hence, the dc-bus capacitive energy y_{Bus} and the supercapacitive energy y_{SC} can be written as

$$y_{\mathrm{Bus}} = \frac{1}{2} C_{\mathrm{Bus}} v_{\mathrm{Bus}}^2 \quad (5)$$

$$y_{\mathrm{SC}} = \frac{1}{2} C_{\mathrm{SC}} v_{\mathrm{SC}}^2 \quad (6)$$

We suppose that there are only static losses in these converters, in which r_{PV}, r_{FC}, r_{Bat}, and r_{SC} represent the only static losses in the PV, the FC, the battery, and the SC converters, respectively. As shown in Fig. 1, the derivative of dc-bus capacitive energy y_{Bus} is given versus p_{PVo}, p_{FCo}, p_{Bato}, p_{SCo}, and p_{Load} by the following differential equation:

$$\dot{y}_{\mathrm{Bus}} = p_{\mathrm{PVo}} + p_{\mathrm{FCo}} + p_{\mathrm{Bato}} + p_{\mathrm{SCo}} - p_{\mathrm{Load}} \quad (7)$$

where

$$p_{\mathrm{PVo}} = p_{\mathrm{PV}} - r_{\mathrm{PV}} \left(\frac{p_{\mathrm{PV}}}{v_{\mathrm{PV}}} \right)^2, \quad (8)$$

$$p_{\mathrm{FCo}} = p_{\mathrm{FC}} - r_{\mathrm{FC}} \left(\frac{p_{\mathrm{FC}}}{v_{\mathrm{FC}}} \right)^2, \quad (9)$$

$$p_{\mathrm{Bato}} = p_{\mathrm{Bat}} - r_{\mathrm{Bat}}\left(\frac{p_{\mathrm{Bat}}}{v_{\mathrm{Bat}}}\right)^2, \tag{10}$$

$$p_{\mathrm{SCo}} = p_{\mathrm{SC}} - r_{\mathrm{SC}}\left(\frac{p_{\mathrm{SC}}}{v_{\mathrm{SC}}}\right)^2, \tag{11}$$

$$p_{\mathrm{Load}} = v_{\mathrm{Bus}} \cdot i_{\mathrm{Load}} = \sqrt{\frac{2y_{\mathrm{Bus}}}{C_{\mathrm{Bus}}}} \cdot i_{\mathrm{Load}} \tag{12}$$

III. Energy Management

In this kind of hybrid system (Fig. 1), there are three variables to be controlled:

- First, the dc bus voltage v_{Bus} (or dc bus energy y_{Bus}) is the most significant variable.
- Second, it is the SC voltage v_{SC} (or supercapacitive energy y_{SC}) (charging supercapacitor).
- Third, it is the battery energy y_{Bat} or the battery state-of-charge *SOC* (charging battery).

and four-control variables:

- the SC power reference p_{SCREF},
- the battery power reference p_{BatREF},
- the FC power reference p_{FCREF}, and
- the PV power reference p_{PVREF}.

A. Literature Review: Energy Management Based on Battery and Supercapacitor Energy Storages

The hybrid power sources based battery and supercapacitor energy storages have already been investigated before recently, for example by Yoo *et al*. [19] who worked on a regulated voltage power sources composed of a diesel engine-based generator, lead acid battery bank, and SC bank for a four-wheel-driven series hybrid electric vehicle (HEV). This vehicle has been designed to operate in two modes: 1). the normal mode utilizing the En-Gen set, SC, and battery, and 2). the EV mode while utilizing the battery and SC. In normal mode, they proposed the dc-link voltage regulated by the SC bank based on a PI-linear controller and battery can assist in the power supply in the normal operation mode to improve the dynamic performance in which the dc–dc converter with the battery bank functions both as the dc-link voltage regulator as well as the current controller to assist with the power supply.

Afterthat, Ongaro *et al.* [20] proposed a power management architecture that utilizes both SC cells and a lithium battery as energy storages for a PV-based wireless sensor network. This work is similar to Yoo's work [19] that also uses the SC bank (2.5 V) to regulate the dc bus voltage of 3.3 V, whereas the PV converter realizes the MPPT of the PV module; the PV converter is controlled by a feedback loop and the reference is determined either by the source MPPT or by the control on the SC voltage, depending on the state of the power management algorithm based on state-machine algorithm. Moreover, the battery converter is a bidirectional boost converter to charge and to utilize the battery (4.2 V) at the same time depending on the working conditions. This choice is dictated by the required voltage level of the battery, respect to the dc power bus.

Afterward, Bambang *et al.* [21] proposed a linear model predictive control (MPC) of FC/battery/SC hybrid source. This work is also similar to You's work [19] that functions based on a dc bus voltage regulation (linear PI controller). However, MPC received a dc bus current reference generated by the dc bus voltage controller; v_{FC}, v_{Bat}, and v_{SC}; and then MPC generates the current references for FC, battery, and SC, in which the dynamic programming is used to find solution for MPC's problem. This seems to have some problems of the online computational burden.

Next, Torreglosa *et al*. [22] proposed the predictive control for the energy management of a FC/battery/SC tramway. Once again, they proposed to use a SC bank to regualte a dc bus voltage of 750 V, where a linear PI controller generates a SC current reference i_{SCREF}. However, the FC and battery current references are estimated by the predictive control algorithm.

The problem of such a control strategy is well known: the online computational burden [21], [22] or the definition of system states (state-machine [20]) implies control algorithm permutations that may lead to a phenomenon of chattering when the system is operating near a border between two states. Solutions exist to avoid such a phenomenon, of course: hard filtering, hysteretic transition, and transition defined by a continuous function.

The hybrid source control strategy presented hereafter is not based on the state definition, so naturally it presents no problem of chattering near state borders. The basic principle here lies in using

- the SCs (the fastest energy source), for supplying energy required to achieve the dc bus stabilization:
  # SCs → DC Bus [19], [20], [21], [22].
- the batteries, for charging the SCs:
  # Battery → SCs
- and, the PV and FC, although obviously the main energy sources of the system, for charging the batteries:
  # PV + FC → Battery

Accordingly, the SC converter is operated to realize a dc link voltage regulation. The battery converter is driven to maintain the SCs at a given state-of-charge, here the SC voltage regulation. Then, the PV and FC converters are also driven to maintain the batteries at a given state-of-charge, here the battery SOC regulation. So, the three-control loops can be seen in Fig. 4.

B. DC Bus Voltage Stabilization

To regulate the dc-bus voltage v_{Bus} (DC link stabilization), based on the flatness control theory [23]–[25], the flat outputs $\boldsymbol{y}$, the control input variables $\boldsymbol{u}$ and the state variables $\boldsymbol{x}$ are defined as

$$y = y_{\mathrm{Bus}},\ u = p_{\mathrm{SCREF}},\ x = v_{\mathrm{Bus}} \tag{13}$$

From (5), the state variable $\boldsymbol{x}$ can be written as

$$x = \sqrt{2y/C_{\mathrm{Bus}}} = \varphi(y). \tag{14}$$

From (7) – (12), the control input variable $\boldsymbol{u}$ can be calculated from the flat output $\boldsymbol{y}$ and its time derivative (named here "*inverse dynamics*"):

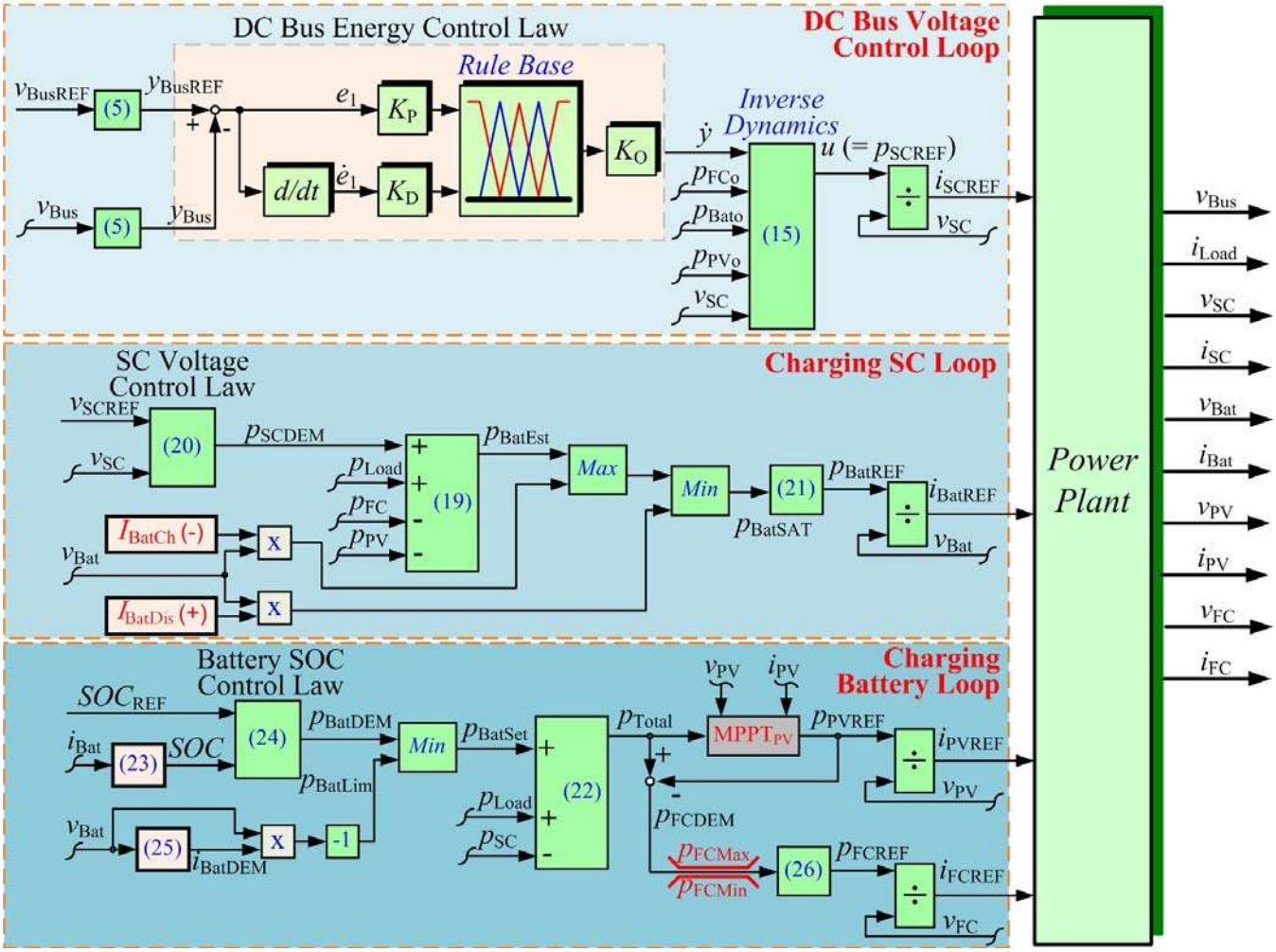

Fig. 4. Control algorithm of FC/PV/Battery/SC power plant.

$$u = 2p_{\mathrm{SCLim}} \cdot \left[1 - \sqrt{1 - \left(\frac{\dot{y} + \sqrt{\frac{2y}{C_{\mathrm{Bus}}}} \cdot i_{\mathrm{Load}} - p_{\mathrm{PVo}} - p_{\mathrm{FCo}} - p_{\mathrm{Bato}}}{p_{\mathrm{SCLim}}} \right)} \right] = \psi(y, \dot{y}) \tag{15}$$

where

$$p_{\mathrm{SCLim}} = v_{\mathrm{SC}}^2 / 4r_{\mathrm{SC}} . \tag{16}$$

p_{SCLim} is the limited maximum power from the SC converter. Thus, it is clear that $x = \varphi(y)$ and $u = \psi(y, \dot{y})$. The proposed reduced order model can be studied as a flat system [23]-[25].

It should note here that the inverse dynamics term (15) is the important expression to prove the system's flatness property; moreover, the differental flatness approach is the model based control, so that p_{PVo}, p_{FCo}, and p_{Bato} are estimated by (8) – (10). The parameter estimation errors [such r_{FC}, r_{SC}, r_{PV}, and r_{Bat} (8)-(11), (16)] will be compensated by the proposed controller presented later. Neverterless, Song *et al*. [26] and Thounthong *et al*. [27] have already shown that the nonlinear differential flatness-based approach provides a robust controller in power electronics applications. The performance of the control system is hardly affected by the error considered in the model parameters.

The control objective is to regulate the dc bus voltage v_{Bus} or the dc bus energy y_{Bus} (= y_1). The controller contains a Takagi-Sugeno (T-S) inference engine and two fuzzy inputs: the energy error e_1 (=$y_{1\mathrm{REF}}$–y_1) and the differential energy error $\dot{e}_1$, which are carefully adjusted using the proportional gain K_{P} and the derivative gain K_{D}, respectively. In addition, the fuzzy output level can be set by the proportional gain K_{O} (Fig. 4) [23].

Triangular and trapezoidal membership functions are chosen for both of the fuzzy inputs, as revealed in Fig. 5(a). There are seven membership functions for each input, including *NB* (Negative Big), *NM* (Negative Medium), *NS* (Negative Small), *Z* (Zero), *PB* (Positive Big), *PM* (Positive Medium) and *PS* (Positive Small). For the singleton output membership function, the zero-order Sugeno model is used, where the membership functions are specified symmetrically [Fig. 5(b)].

This article has been accepted for publication in a future issue of this journal, but has not been fully edited. Content may change prior to final publication. Citation information: DOI 10.1109/TIA.2016.2581138, IEEE Transactions on Industry Applications

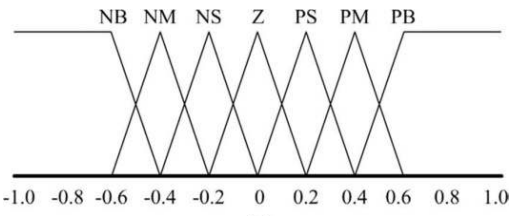

$\dot{e}$ \ e	NB	NM	NS	Z	PS	PM	PB
NB	PB	PB	PB	PB	PB	PB	PM
NM	PB	PB	PB	PM	PM	PM	PM
NS	PM	PM	PM	PS	PS	Z	Z
Z	PB	PM	PS	Z	NS	NM	NB
PS	Z	Z	NS	NS	NM	NM	NM
PM	NM	NM	NM	NM	NB	NB	NB
PB	NM	NB	NB	NB	NB	NB	NB

(c)

Fig. 5. Rule base and membership functions. (a) Input membership functions. (b) Output membership function. (c) Rule base.

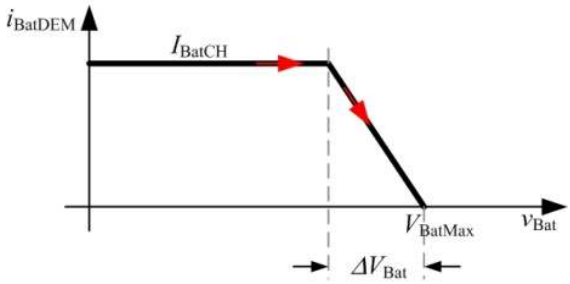

Fig. 6. Battery charging limitation function.

For the rule base, expert suggestions, an experimental approach, and a trial and error technique were used to define the relationships between the inputs and the output. The data representation was in the form of an *IF-THEN* rule, as shown in the following example:

IF e_{1i} *is NS and* $\dot{e}_{1i}$ *is NS*
THEN z_i *(=output) is NB.*

As shown in Fig. 5(c), the total number of rule bases is therefore equal to 49 rules. To obtain the output of the controller, the center of gravity method for the *COGS* of the singletons is utilized as

$$U = \frac{\sum_{i=1}^{N} w_i z_i}{\sum_{i=1}^{N} w_i} \tag{17}$$

where the weights (w_i) can be retrieved from

$$w_i = \mathbf{max}\left(e_{1i}, \dot{e}_{1i}\right). \tag{18}$$

C. Charging Supercapacitor

To charge the SC module by the battery bank, equation (7) may be written with y_{Bus} = constant and without losses (Fig. 1) as

$$p_{SC} + p_{Load} = p_{PV} + p_{FC} + p_{Bat} \tag{19}$$

A desired SC voltage reference is defined as v_{SCREF}. A proportional (P) controller is chosen, so that it generates the SC power demand p_{SCDEM}:

$$p_{SCDEM} = K_{SC}\left(v_{SCREF} - v_{SC}\right) \tag{20}$$

where K_{SC} is the controller parameter. Refer to (19), this signal p_{SCDEM} becomes p_{BatEst}. To protect the battery bank, the battery current must be limited within an interval [limit charging current I_{BatCh} (here negative value), limit discharging current I_{BatDis} (here positive value). Subsequently, the signal p_{BatEst} must be limited by using maximum and minimum functions. This results in p_{BatSAT}. To optimize the lifetime of the batteries, it is advisable to limit the battery current (or power) slope in order to ensure a longer battery lifetime. Therefore, a first-order filter is chosen for the battery power dynamics as follow:

$$p_{BatREF}(t) = p_{BatSAT}(t) \cdot (1 - e^{-\frac{t}{\tau_1}}) \tag{21}$$

where, τ_1 is the regulation parameters.

D. Charging Li-Ion Battery

To charge the battery, equation (7) may be written with y_{Bus} = constant and without losses (Fig. 1) as

$$p_{Bat} + p_{Load} = \overbrace{p_{PV} + p_{FC}}^{p_{Total}} + p_{SC} \tag{22}$$

The familiar battery *SOC* estimation is defined as [28]

$$SOC(t) = SOC_o + \frac{1}{Q_{Bat}} \int_{t_o}^{t} i_{Bat}(\tau) d\tau \tag{23}$$

where SOC_o is the known battery *SOC* [%] at the time t_o, and Q_{Bat} is the rated capacity [Ah]. The simple method to charge the battery is via the constant current approach (maximum charging current I_{BatCH} is set to approximately $Q_{Bat}/2$ - $Q_{Bat}/5$; for a Li-ion battery, it can be set at $I_{BatCH} = Q_{Bat}$) when the *SOC* is far from the state of charge reference SOC_{REF}, the use of a reduced current when the *SOC* is near SOC_{REF}, and zero when the *SOC* is equal to SOC_{REF} [29]. Then, a proportional (P) controller is chosen, so that it generates the battery power demand p_{BatDEM}:

$$p_{BatDEM} = K_{Bat}\left(SOC_{REF} - SOC\right) \tag{24}$$

where K_{Bat} is the controller parameter. Then, p_{BatSet} = ***min***$[p_{BatDEM}, p_{BatLim}]$, in which p_{BatLim} is generated by $v_{Bat} \times i_{BatDEM}$. To avoid overvoltage during charging battery in case

of an erroneous *SOC* estimation, the battery voltage must be monitored to limit charging current. Thus, i_{BatDEM} is the charging limitation function (Fig. 6) generated by

$$i_{\text{BatDEM}} = I_{\text{BatCh}} \cdot \boldsymbol{min}\left(1, \frac{V_{\text{BatMax}} - v_{\text{Bat}}}{\Delta V_{\text{Bat}}}\right) \qquad (25)$$

where V_{BatMax} is the defined maximum battery voltage, and ΔV_{Bus} is the defined voltage band.

Therefore, the system generates a total power reference p_{Total}. First, p_{Total} is considered as the PV power. The power must be limited in level, within an interval of the maximum of p_{PVMax} (maximum power point tracking MPPT_{PV} [30], [31]; here, the perturb and observe (P&O) algorithm [32], [33] has been implemented) and the minimum of p_{PVMin} (set to 0 W). Second, the difference between p_{Total} and p_{PVREF} is the FC power demand p_{FCDEM}. The FC power must be limited in level, within an interval of the maximum p_{FCMax} and the minimum p_{FCMin} (set to 0 W), and limited in dynamics with respect to the constraints that are associated with the FC [34], [35]. Then, to limit the transient FC power, a second order filter is used [36], [37], such that the power demand p_{FCDEM} is always limited by

$$p_{\text{FCREF}}(t) = p_{\text{FCDEM}}(t) \cdot \left(1 - e^{-\frac{t}{\tau_2}} - \frac{t}{\tau_2} e^{-\frac{t}{\tau_2}}\right) \qquad (26)$$

where τ_2 is the control parameter. So, the proposed control algorithm is portrayed in Fig. 4.

IV. Experimental Validation

The experimental tests were performed by connecting a dc bus voltage of 60 V loaded by an electronic load. The parameters associated with the system regulation loops are summarized in Table I. The test bench details can be seen in Appendix. Note that equipvalent series resistances in these converters are obtained from the offline identification. The proposed control loops (Fig. 4) were implemented in the real-time card dSPACE DS1104 platform using the fourth-order Runge–Kutta integration algorithm and a sampling time of 100 μs, through the mathematical environment of MATLAB–Simulink.

Firstly, for the sake of the dc-bus voltage stabilization by the supercapacitor module, the oscilloscope waveforms in Figs. 7 and 8 portray the dynamic characteristics that are obtained during the large load step of 300 W and 490 W, respectively. It shows the dc-bus voltage, the load power (disturbance), the SC power, and the SC voltage. The initial state is in no-load power; the SC storage device is full of charge, i.e., the SC voltage = 25 V (v_{SCREF} = 25 V); the battery is full of charge (95 % here), and the dc-bus voltage is regulated at 60 V (v_{BusREF} = 60 V); as a result, the FC, PV, battery and SC powers are zero. After that, one sets p_{FCREF} = p_{PVREF} = p_{BATREF} = 0 in order to observe the only SC to stabilize the dc bus voltage. At t = 20 ms, the large load power steps from 0 W to a constant value (positive transition). One can see the SC supplies the transient and steady-state load power demand and the similar waveforms in Figs. 7 and 8. The dc-bus voltage (dc-link stabilization) is minimally influenced by the large load power step.

TABLE I
System Parameters

v_{BusREF}	60	V
v_{SCREF}	25	V
SOC_{REF}	95%	
K_{P}	0.185	
K_{D}	$0.115\text{x}10^{-3}$	
K_{O}	-260	
K_{SC}	270	
τ_1	1	s
K_{Bat}	100	
τ_2	5	s
ΔV_{Bat}	1	V
V_{BatMax}	26	V
I_{BatCH}	–4	A
I_{BatDis}	+8	A
P_{FCMax}	550	W
P_{FCMin}	0	W
P_{PVMin}	0	W
C_{Bus}	8,000	μF
r_{FC}	0.13	Ω
r_{PV}	0.14	Ω
r_{Bat}	0.18	Ω
r_{SC}	0.18	Ω

Next, Fig. 9 presents waveforms that are obtained during the long load cycles. The load will be varied to emulate the real environment: light load, over load, and transient transitions. Note that the PV array is installed on the roof of the laboratory building, so that the solar energy production is directly from the sun.

The graph shows the dc bus voltage, the PV voltage, the FC voltage, the load power, the SC power, the battery power, the PV power, the FC power, the battery current, the FC current, the SC voltage, the battery voltage, and the battery SOC.

In the initial state, the load power is zero; the battery is full of charge, i.e., $SOC = SOC_{\text{REF}}$ = 95%; and the SC is also full of charge, i.e., $v_{\text{SC}} = v_{\text{SCREF}}$ = 25 V; as a result, the PV, FC, battery, and SC powers are zero.

At t_1, the load power steps from 0 W to the constant power of 500 W. The following observations are made:

- The SC supplies most of the transient step load.
- At the same time, the PV power increases to a maximum power point (MPP) of approximately 400 W at t_2, which is limited by the maximum power point tracker (MPPT). Due to a cloudy sky during the test bench validation, the MPP is only 400 W instead of its rated PV power 800 W.
- Simultaneously, the FC and battery powers increase with limited dynamics [refer to (21) and (26)] to the small constant power at t_2.
- The input from the SC, which supplies most of the transient power that is required during the stepped load, slowly decreases to zero.

Next, at t_3, the large load power steps from 500 W to the constant power of 1,400 W. The following clarifications are made:

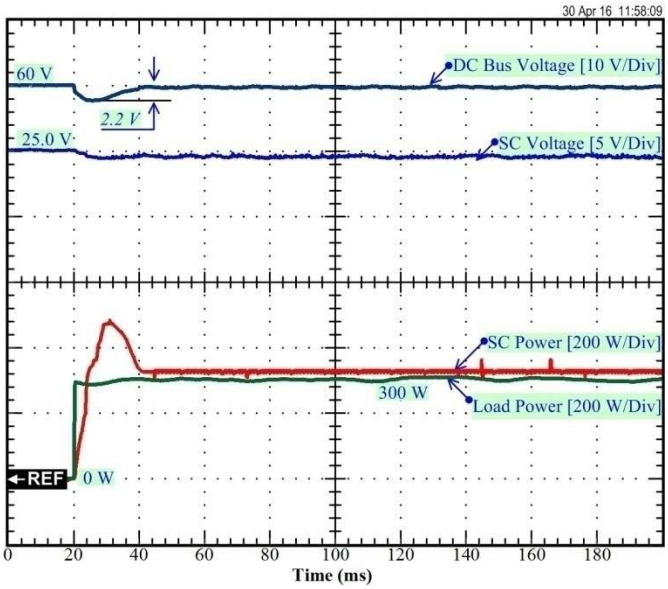

Fig. 7. Experimental results: Dynamic characteristic of the hybrid source during a step load from 0 to 300 W.

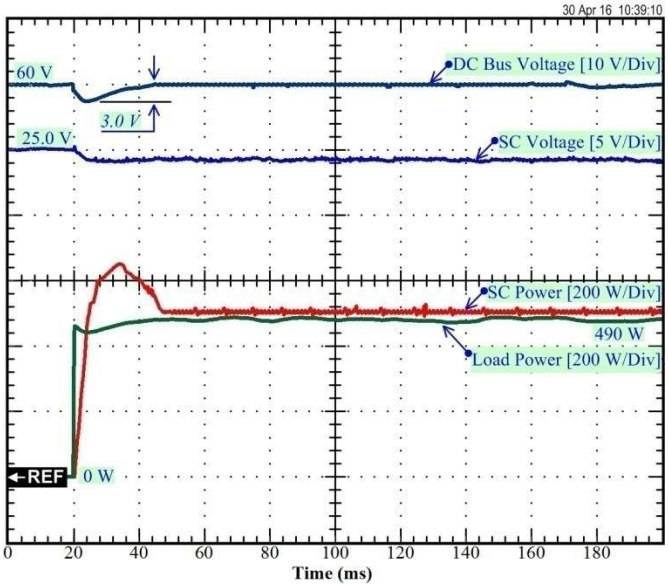

Fig. 8. Experimental results: Dynamic characteristic of the hybrid source during a step load from 0 to 490 W.

- The PV power is still at the maximum power level of 400 W by the $MPPT_{PV}$.
- The SC supplies most of the transient step load.
- The battery is deeply discharged with limited dynamics [refer to (21)] to its limited discharging current at −8 A at t_4.
- Simultaneously, the FC power increases with limited dynamics [refer to (26)] to its limited maximum power of 550 W at t_5.
- The input from the SC, which supplies most of the transient power that is required during the stepped load, slowly decreases, and the unit remains in a discharge state after the load step because the steady-state load power (1,400 W) is greater than the total power supplied by the PV, FC, and battery.

Subsequently, at t_6, the load power steps from 1,400 W to zero, and SOC_{REF} (= 95%) > SOC (= 93%); v_{SCREF} (= 25 V) > v_{SC} (= 16 V). As a result, the SC changes its state from discharging to charging, demonstrating the six phases.

- First, the PV still supplies its limited maximum power of around 400 W; the FC still supplies its limited maximum power of 550 W; and the battery supplies its limited discharging current of +8 A. This means the PV, FC, and battery supply powers to charge only the SC.
- Second, at t_7 (v_{SC} = 21 V), the SC is nearly charged at 25 V, which afterward reduces the charging power. As a result, the FC and battery powers are reduced. But, the PV still supplies its limited maximum power of around 400 W.
- Third, at t_8 (SOC = 92.8 %), the battery changes its state from discharging to charging. This means the PV and FC supply powers to charge both the SC and battery, intelligently.
- Forth, at t_9, the FC power reduces to zero, so that only the PV supplies power to charge both the SC and battery. Simultaneously, the PV power is gradually reduced.
- Fifth, at t_{10}, the battery is charged at its limited charging current of –4 A.
- Sixth, at t_{11}, the SC is fully charged at 25 V; then, the SC power is zero. At the same time, the battery is nearly charged at 94%, which subsequently reduces the charging current. Finally, the battery will be charged by the PV to full-of-charge.

Finally, Fig. 10 presents waveforms that are obtained during the short load cycles. The graph shows the dc bus voltage, the FC voltage, the PV voltage, the load power, the SC power, the battery power, the PV power, the FC power, the battery current, the FC current, the battery voltage, the SC voltage, and the battery SOC. In the initial state, the load power is zero, and the storage devices are fully charge, i.e., v_{SC} = 25 V and battery SOC = 95%; as a result, the FC, PV, SC, and battery powers are zero. At t_1 (t = 40 s), the load power steps to the final constant power of around 1300 W. The following observations are made:

- The SC supplies most of the 1300W power that is required during the transient step load.
- Synchronously, the battery power increases with limited dynamics [refer to equ. (21)] to a limited discharge current of +8 A (= I_{BatDis}) at t_2.
- Simultaneously, the PV power increases to a maximum power point (MPP) of around 400 W at t_3, which is limited by its MPPT automatically.
- Concurrently, the FC power increases with limited dynamics [refer to equ. (26)] to a maximum power of 550 W at t_4.

This article has been accepted for publication in a future issue of this journal, but has not been fully edited. Content may change prior to final publication. Citation information: DOI 10.1109/TIA.2016.2581138, IEEE Transactions on Industry Applications

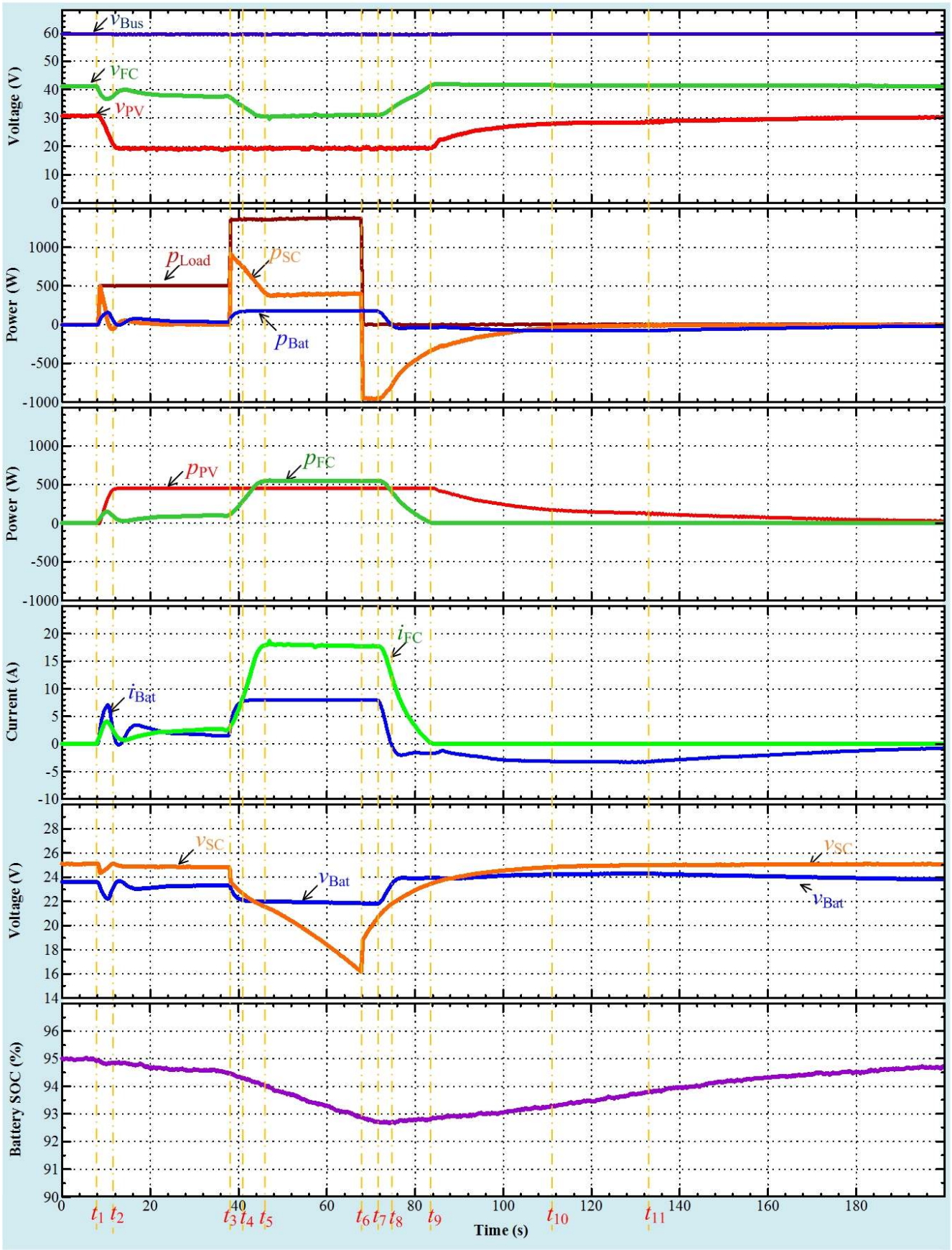

Fig. 9. Experimental results: power plant response during long load cycles.

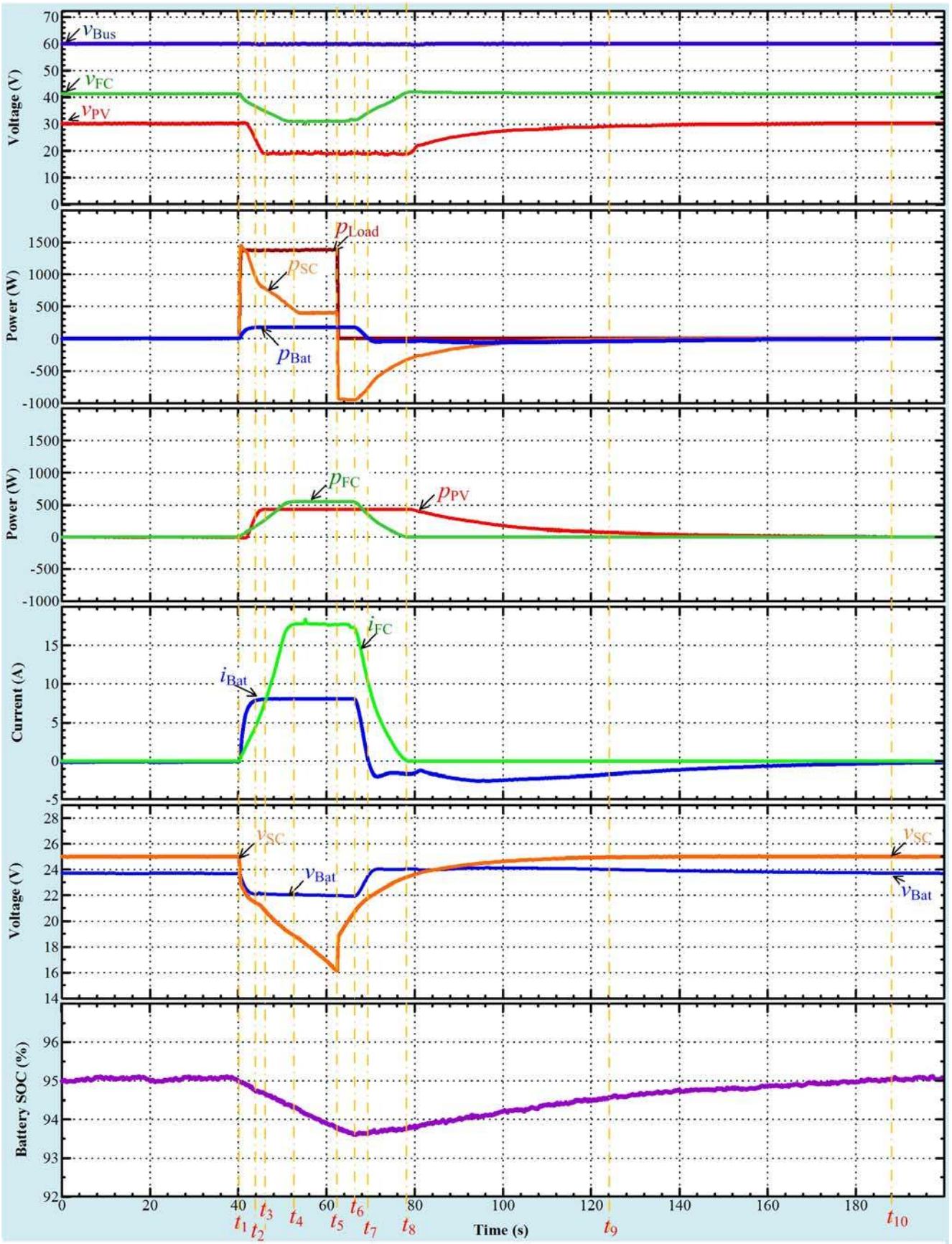

Fig. 10. Experimental results: power plant response during short load cycles.

- The input from the SC, which supplies most of the transient power that is required during the stepped load, slowly decreases and the unit remains in a discharge state after the load step because the steady-state load power (approximately 1300W) is greater than the total power supplied by the FC, PV, and battery.

Subsequently, at t_5, the load power steps from 1,300 W to zero, and battery SOC_{REF} (= 95%) > SOC (= 93.7%); v_{SCREF} (= 25 V) > v_{SC} (= 16 V). As a result, the SC changes its state from discharging to charging, demonstrating the six phases.

- First, the PV still supplies its limited maximum power of around 400 W; the FC still supplies its limited maximum power of 550 W; and the battery supplies its limited discharging current of +8 A. This means the PV, FC, and battery supply powers to charge only the SC.
- Second, at t_6 (v_{SC} = 21 V), the SC is nearly charged at 25 V, which afterward reduces the charging power. As a result, the FC and battery powers are reduced. But, the PV still supplies its limited maximum power of around 400 W.
- Third, at t_7 (SOC = 93.7 %), the battery changes its state from discharging to charging. This means the PV and FC supply powers to charge both the SC and battery, intelligently.
- Forth, at t_8, the FC power reduces to zero, so that only the PV supplies power to charge both the SC and battery. Simultaneously, the PV power is gradually reduced.
- Fifth, at t_9, the battery is charged at small current; the SC is fully charged at 25 V; then, the SC power is zero.
- Sixth, at t_{10}, the battery is fully charged at 95%; then, the FC, PV, SC, and battery powers are zero.

One can observe that the power plant is always energy balanced ($p_{Load} = p_{PV} + p_{FC} + p_{Bat} + p_{SC}$) when using the proposed original control algorithm.

V. Conclusion

The main contribution of this present work is to propose an original control algorithm for a dc distributed generation supplied by the PV/FC sources, and the storage devices: SCs and Li-Ion battery. The combined utilization of batteries and SCs is the perfect hybridization system of a high energy and high power density. The control structure presents how to avoid from the fast transition of the battery and FC powers, and then reducing the battery and FC stresses. As a result, hybrid power source will increase its lifetime. However, it is beyond the scope of this paper to demonstrate the power sources lifetime.

Experimental results in our laboratory carried out using a small-scale test bench, which employs a PEMFC (1.2 kW, 46 A), a PV (800 W, 31 A) and storage devices composed of SC bank (100 F, 32 V) and Li-Ion battery module (11.6 Ah, 24 V), corroborate the excellent performances of the proposed energy management during load cycles.

Finally, the nonlinear flatness-based control is a model based control approach. It requires to know system parameters (such r_{FC}, r_{SC}, etc…) to obtain the differential flatness property [refer to the dynamics term (15)]. For future works, some online state-observers (or parameter-observers) [38] will be used to improve the system performances.

Appendix. Test Bench Description of the Power Plant

The prototype test bench of the studied power plant was implemented in the laboratory, as illustrated in Fig. 11. The prototype PV converter of 2 kW, the FC converter of 2 kW, the battery converter of 4 kW, and the SC converter of 4 kW, were realized in the RERC laboratory (Fig. 11). Details of the real power sources and storage devices are presented in Table II.

The PV, FC, battery, and SC current regulation loops were realized by analog circuits as inner current control loops. The control algorithms (external control loops), which generate the current references, were implemented in the real time card dSPACE DS1104 (as presented in Fig. 11).

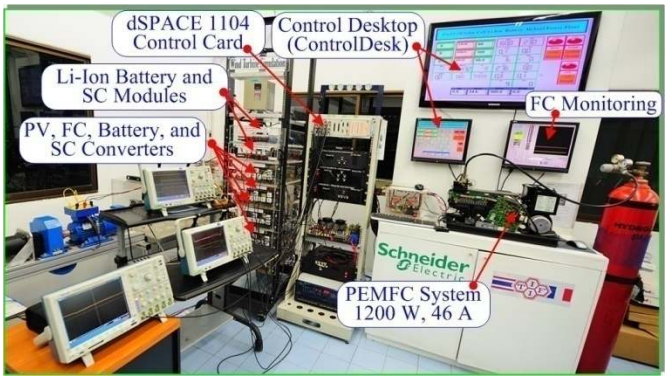

Fig. 11. Photograph of the experimental setup in the laboratory (Renewable Energy Research Centre, KMUTNB).

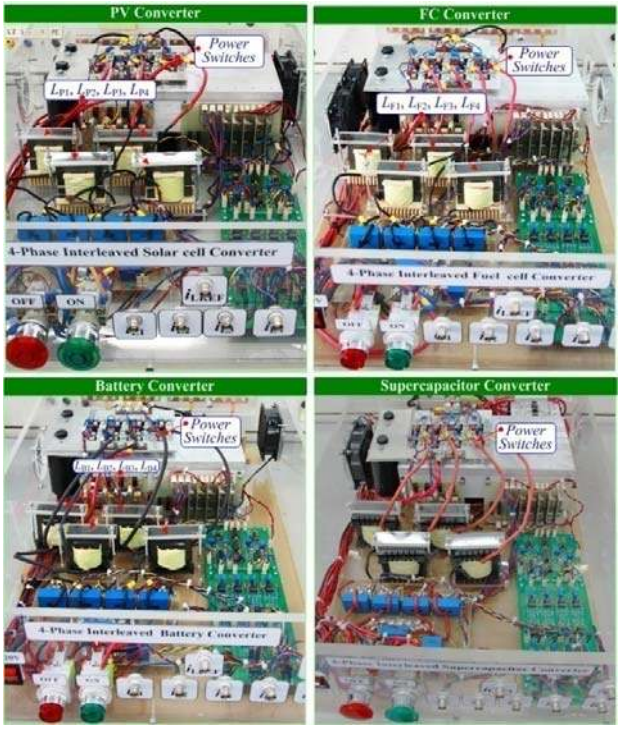

Fig. 12. Photograph of the implement converters.

Table II.
SPECIFICATIONS OF THE STORAGE DEVICES AND THE POWER SOURCES

Fuel Cell System (by Ballard Power Systems Inc):		
Rated Power	1,200	W
Rated Current	46	A
Rated Voltage	26	V
Photovoltaic Array (by Ekarat Solar Company):		
Number of Panels in Parallel	4	
Panel Open Circuit Voltage	33.5	V
Panel Rated Voltage	26	V
Panel Rated Current	7.7	A
Panel Rated Power	200	W
Array Rated Power	800	W
Li-Ion Battery Bank (by SAFT Technologies Company):		
Number of Cells in Series	6	
Number of String in Parallel	2	
Cell Maximum Voltage	4.2	V
Bank Capacity (C_{Bat})	11.6	Ah
Bank Maximum Voltage	24	V
Supercapacitor Bank (by Maxwell Technologies):		
Number of Cells in Series	12	
Cell Capacity	1,200	F
Cell Maximum Voltage	2.7	V
Bank Capacity (C_{Bat})	100	F
Bank Maximum Voltage	32	V

REFERENCES

[1] Ching-Tsai Pan, Ming-Chieh Cheng, Ching-Ming Lai, and Po-Yen Chen, "Current-Ripple-Free Module Integrated Converter With More Precise Maximum Power Tracking Control for PV Energy Harvesting," *IEEE Trans. Ind. Appl*., vol. 51, no. 1, pp. 271–278, Jan./Feb. 2015.

[2] S. A. Saleh, A. S. Aljankawey, B. Alsayid, and M. S. Abu-Khaizaran, "Influences of Power Electronic Converters on Voltage–Current Behaviors During Faults in DGUs—Part II: Photovoltaic Systems," *IEEE Trans. Ind. Appl*., vol. 51, no. 4, pp. 2832–2845, July/Aug. 2015.

[3] C. K. Sundarabalan and K. Selvi, "Compensation of voltage disturbances using PEMFC supported Dynamic Voltage," *Int. J. Electrical Power & Energy Systems*, vol. 71, pp. 77–92, Oct. 2015.

[4] N. Bizon, "Improving the PEMFC energy efficiency by optimizing the fueling rates based on extremum seeking algorithm," *Int. J. Hydrogen Energy*, vol. 39, no. 20, pp. 10641–10654, July 2014.

[5] P. Thounthong, L. Piegari, S. Pierfederici, and B. Davat, "Nonlinear intelligent DC grid stabilization for fuel cell vehicle applications with a supercapacitor storage device," *Int. J. Electrical Power & Energy Systems*, vol. 64, pp. 723–733, Jan. 2015.

[6] K. Vijayaraghavan, J. DeVaal, and M. Narimani, "Dynamic model of oxygen starved proton exchange membrane fuel-cell using hybrid analytical-numerical method," *J. Power Sources*, vol. 285, pp. 291–302, July 2015.

[7] Jianwu Zeng, Wei Qiao, and Liyan Qu, "An Isolated Three-Port Bidirectional DC–DC Converter for Photovoltaic Systems With Energy Storage," *IEEE Trans. Ind. Appl*., vol. 51, no. 4, pp. 3493–3503, July/Aug. 2015.

[8] A. Tani, M. B. Camara, and B. Dakyo, "Energy Management in the Decentralized Generation Systems Based on Renewable Energy—Ultracapacitors and Battery to Compensate the Wind/Load Power Fluctuations," *IEEE Trans. Ind. Appl*., vol. 51, no. 2, pp. 1817–1827, Mar./Apr. 2015.

[9] Zong Yu Gao, Jian Jun Fang, Yi Nong Zhang, Lan Jiang, Di Sun, and Wenrong Guo, "Control of urban rail transit equipped with ground-based supercapacitor for energy saving and reduction of power peak demand," *Int. J. Electrical Power & Energy Systems*, vol. 67, pp. 439–447, May 2015.

[10] A. Abdelkafi and L. Krichen, "Energy management optimization of a hybrid power production unit based renewable energies," *Int. J. Electrical Power & Energy Systems*, vol. 62, pp. 1–9, Nov. 2014.

[11] N. Devillers, M.C. Péra, D. Bienaimé, and M. L. Grojo, "Influence of the energy management on the sizing of Electrical Energy Storage Systems in an aircraft," *J. Power Sources*, vol. 270, pp. 391–402, Dec. 2014.

[12] Hongjie Jia, Yunfei Mu, and Yan Qi, "A statistical model to determine the capacity of battery–supercapacitor hybrid energy storage system in autonomous microgrid," *Int. J. Electrical Power & Energy Systems*, vol. 54, pp. 516–524, Jan. 2014.

[13] V. Samavatian and A. Radan, "A high efficiency input/output magnetically coupled interleaved buck–boost converter with low internal oscillation for fuel-cell applications: Small signal modeling and dynamic analysis," *Int. J. Electrical Power & Energy Systems*, vol. 67, pp. 261–271, May 2015.

[14] P. Thounthong, P. Tricoli, and B. Davat, "Performance investigation of linear and nonlinear controls for a fuel cell/supercapacitor hybrid power plant," *Int. J. Electrical Power & Energy Systems*, vol. 54, pp. 454–464, Jan. 2014.

[15] K. J. Hartnett, J. G. Hayes, M. S. Rylko, B. J. Barry, and J. W. Maslon, "Comparison of 8-kW CCTT IM and Discrete Inductor Interleaved Boost Converter for Renewable Energy Applications," *IEEE Trans. Ind. Appl*., vol. 51, no. 3, pp. 2455–2469, May./June 2015.

[16] Choi Hyuntae, M. Ciobotaru, Jang Minsoo, and V. G. Agelidis, "Performance of Medium-Voltage DC-Bus PV System Architecture Utilizing High-Gain DC–DC Converter," *IEEE Trans. Sustainable Energy*, vol. 6, no. 2, pp. 464–473, April 2015.

[17] Kai-Wei Hu, Jung-Chi Wang, Tsai-Sheng Lin, and Chang-Ming Liaw, "A Switched-Reluctance Generator With Interleaved Interface DC–DC Converter," *IEEE Trans. Energy Convers*., vol. 30, no. 1, pp. 273–284, Mar. 2015.

[18] W. Thammasiriroj, V. Chunkag, M. Phattanasak, S. Pierfederici, B. Davat, and P. Thounthong, "Nonlinear single-loop control of the parallel converters for a fuel cell power source used in DC grid applications," *Int. J. Electrical Power & Energy Systems*, vol. 65, pp. 41–48, Feb. 2015.

[19] Hyunjae Yoo, Seung-Ki Sul, Yongho Park, and Jongchan Jeong, "System Integration and Power-Flow Management for a Series Hybrid Electric Vehicle Using Supercapacitors and Batteries," *IEEE Trans. Ind. Appl*., vol. 44, no. 1, pp. 108–114, Jan./Feb. 2008.

[20] F. Ongaro, S. Saggini, and P. Mattavelli, "Li-Ion Battery-Supercapacitor Hybrid Storage System for a Long Lifetime, Photovoltaic-Based Wireless Sensor Network," *IEEE Trans. Power Electron*., vol. 27, no. 9, pp. 3944–3951, Sep. 2012.

[21] A. R. T. Bambang, A. S. Rohman, C. J. Dronkers, R. Ortega, and A. Sasongko, "Energy Management of Fuel Cell/Battery/Supercapacitor Hybrid Power Sources Using Model Predictive Control," *IEEE Trans. Ind. Informat*., vol. 10, no. 4, pp. 1992–2002, Nov. 2014.

[22] J. P. Torreglosa, P. García, L. M. Fernández, and F. Jurado, "Predictive Control for the Energy Management of a Fuel-Cell–Battery–Supercapacitor Tramway," *IEEE Trans. Ind. Informat*., vol. 10, no. 1, pp. 276–285, Feb. 2014.

[23] P. Thounthong, A. Luksanasakul, P. Koseeyaporn, and B. Davat, "Intelligent model-based control of a standalone photovoltaic/fuel cell power plant with supercapacitor energy storage," *IEEE Trans. Sustain. Energy*, vol. 4, no. 1, pp. 240–249, Jan. 2013.

[24] P. Thounthong, S. Sikkabut, P. Mungporn, L. Piegari, B. Nahid-Mobarakeh, S. Pierfederici, and B. Davat, "DC Bus Stabilization of Li-Ion Battery Based Energy Storage for a Hydrogen/Solar Power Plant for Autonomous Network Applications," *IEEE Trans. Ind. Appl*., vol. 51, no. 4, pp. 2717–2725, July/Aug. 2015.

[25] A. Battiston et *al.*, "A control strategy for electric traction systems using a PM-motor fed by a bidirectional z-source inverter," *IEEE Trans. Veh. Technol*., vol. 63, no. 9, pp. 4178–4191, Nov. 2014.

[26] E. Song, A. F. Lynch, and V. Dinavahi, "Experimental validation of nonlinear control for a voltage source converter," *IEEE Trans. Control Syst. Technol*., vol. 17, no. 5, pp. 1135–1144, Sep. 2009.

[27] P. Thounthong, S. Pierfederici, and B. Davat, "Analysis of differential flatness-based control for a fuel cell hybrid power source," *IEEE Trans.Energy Convers*., vol. 25, no. 3, pp. 909–920, Sep. 2010.

[28] Qi Li, Weirong Chen, Zhixiang Liu, Ming Li, and Lei Ma, "Development of energy management system based on a power sharing strategy for a fuel cell-battery-supercapacitor hybrid tramway," *J. Power Sources*, vol. 279, pp. 267–280, April 2015.

[29] P. Thounthong, S. Raël, and B. Davat, "Control algorithm of fuel cell and batteries for distributed generation system," *IEEE Trans. Energy Convers.*, vol. 23, no. 1, pp. 148–155, Mar. 2008.
[30] A. Elrayyah, Y. Sozer, and M. Elbuluk, "Microgrid-Connected PV-Based Sources: A Novel Autonomous Control Method for Maintaining Maximum Power," *IEEE Industry Applications Magazine*, vol. 21, no. 2, pp. 19–29, Mar/Apr. 2015.
[31] G. Spagnuolo, G. Petrone, B. Lehman, C. A. R. Paja, Y. Zhao, and M. L. O. Gutierrez, "Control of Photovoltaic Arrays: Dynamical Reconfiguration for Fighting Mismatched Conditions and Meeting Load Requests," *IEEE Industrial Electronics Magazine*, vol. 9, no. 1, pp. 62–76, March 2015.
[32] Makoto Uoya and Hirotaka Koizumi, "A Calculation Method of Photovoltaic Array's Operating Point for MPPT Evaluation Based on One-Dimensional Newton–Raphson Method," *IEEE Trans. Ind. Appl.*, vol. 51, no. 1, pp. 567–575, Jan./Feb. 2015.
[33] M. Killi and S. Samanta, "Modified Perturb and Observe MPPT Algorithm for Drift Avoidance in Photovoltaic Systems," *IEEE Trans. Ind. Electron*., vol. 62, no. 9, pp. 5549–5559, Sep. 2015.
[34] P. Thounthong and B. Davat, "Study of a multiphase interleaved stepup converter for fuel cell high power applications,," *Energy Convers. Manage.*, vol. 51, no. 4, pp. 826–832, Apr. 2010.
[35] P. Thounthong and S. Pierfederici, "A new control law based on the differential flatness principle for multiphase interleaved DC–DC converter," *IEEE Trans. Circuits Syst. II, Exp. Briefs*, vol. 57, no. 11, pp. 903–907, Nov. 2010.
[36] M. Phattanasak, R. Gavagsaz-Ghoachani, J.-Ph. Martin, B. Nahid-Mobarakeh, S. Pierfederici, and B. Davat, "Control of a Hybrid Energy Source Comprising a Fuel Cell and Two Storage Devices Using Isolated Three-Port Bidirectional DC–DC Converters," *IEEE Trans. Ind. Appl*., vol. 51, no. 1, pp. 491–497, Jan./Feb. 2015.
[37] P. Thounthong, "Control of a three-level boost converter based on a differential flatness approach for fuel cell vehicle applications", *IEEE Trans. Veh. Technol*., vol. 61, no. 3, pp. 1467-1472, March 2012.
[38] H. Renaudineau, J.-Ph. Martin, B. Nahid-Mobarakeh and , S. Pierfederici, " DC–DC Converters Dynamic Modeling With State Observer-Based Parameter Estimation ", *IEEE Transactions on Power Electronics*, vol. 30, no. 6, pp. 3356-3363, June 2015.

Suwat Sikkabut received the B.S. and M.E. degrees in electrical engineering from King Mongkut's University of Technology North Bangkok (KMUTNB), Bangkok, Thailand, in 2008 and 2016, respectively.

Currently, he is a researcher in Thai-French Innovation Institute, King Mongkut's University of Technology North Bangkok. His current research interests include power electronics, and electrical devices (Fuel cells, Solar cell, batteries, and supercapacitors).

Pongsiri Mungporn received the B.S. and M.E. degrees in electrical engineering from King Mongkut's University of Technology North Bangkok (KMUTNB), Bangkok, Thailand, in 2008 and 2016, respectively.

Currently, he is a researcher in Thai-French Innovation Institute, King Mongkut's University of Technology North Bangkok. His current research interests include power electronics, and electrical devices (Fuel cells, Solar cell, batteries, and supercapacitors).

Chainarin Ekkaravarodome (S'09–M'10) received the B.Ind.Tech in Industrial Electrical Technology from King Mongkut's Institute of Technology North Bangkok (KMITNB), Bangkok, Thailand, in 2003, and his M.E. and Ph.D. in Electrical Engineering and Energy Technology from King Mongkut's University of Technology Thonburi (KMUTT), Bangkok, Thailand, in 2005 and 2009, respectively.

He is currently a Lecturer with the Department of Instrumentation and Electronics Engineering, Faculty of Engineering, King Mongkut's University of Technology North Bangkok (KMUTNB). His current research interests include electronic ballasts, LED drivers, power-factor-correction circuits, resonant rectifiers, and soft-switching power converters.

Nicu Bizon (M'06), was born in Albesti de Muscel, Arges county, Romania, 1961. He received the B.S. degree in electronic engineering from the University "Polytechnic" of Bucharest, Romania, in 1986, and the PhD degree in Automatic Systems and Control from the same university, in 1996.

From 1996 to 1989, he was in hardware design with the Dacia Renault SA, Romania. He is currently professor with the University of Pitesti, Romania, and dean of the Faculty of Electronics, Communication and Computers from 2012. He is editor of six books and more than 300 papersin related fields to Energy, which is his current research interest.

Pietro Tricoli (M'06) was born in Naples, Italy, on September 8, 1978. He received the M.S. and Ph.D. degrees in Electrical Engineering from the University of Naples Federico II, Italy, in 2002 and 2005, respectively.

He is currently a Lecturer of Electrical Power and Control in the Department of Electronic, Electrical, and Systems Engineering, University of Birmingham, Birmingham, U.K. He is the author of more than 60 scientific papers published in international journals and conference proceedings. His research interests include storage devices for road electric vehicles, railways, and rapid transit systems, wind and photovoltaic generation, railway electrification systems and modeling and control of multilevel converters. Dr. Tricoli is a member of the IEEE Industrial Electronics Society and member of the IET Midlands Power Group. He is the Web & Publication Chair of the International Conference on Clean Electrical Power. He is a Registered Professional Engineer in Italy.

Babak Nahid-Mobarakeh (M'05–SM'12) received the Ph.D. degree in electrical engineering from the Institut National Polytechnique de Lorraine (INPL), Nancy, France, in 2001.

From 2001 to 2006, he was with the Centre de Robotique, Electrotechnique et Automatique, University of Picardie, Amiens, France, as an Assistant Professor. In September 2006, he joined the École Supérieure d'Electricité et de Mécanique, Université de Lorraine, where he is currently an Associate Professor. He is also with the Groupe de Recherche en Electrotechnique et Electronique de Nancy, University of Lorraine. He is the author or coauthor of more than 100 international journals and conference papers. His main research interests include nonlinear and robust control techniques applied to electric systems, fault detection and fault-tolerant control of power systems, and stabilization of microgrids.

Dr. Nahid-Mobarakeh was the recipient of the Best Paper Prize of the IEEE Transportation Electrification Conference in 2013 and the Second Best Paper Prize of the IEEE Industry Applications Society-Industrial Automation and Control Committee in 2010.

Serge Pierfederici received the Engineer degree from École Nationale Supérieure en Électricité et Mécanique (ENSEM), Nancy-Lorraine, France, in 1994, the Ph.D. degree (electrical engineering) and the Habilitation à Diriger des Recherches degree (HDR) from the Institut National Polytechnique de Lorraine (INPL), Nancy-Lorraine, France, in 1998 and 2007, respectively.

Since 2009, he has been a Professor in Université de Lorraine. His research include the stability study of distributed power systems, the modeling and the control of power electronic converters.

Bernard Davat (M'89) received the Engineer degree from Ecole Nationale Supérieure d'Electrotechnique, d'Electronique, d' Informatique, d'Hydraulique et des Telecommunications (ENSEEIHT), Toulouse, France, in 1975, and the Ph.D. and Docteur d'Etat degrees in elecrical engineering from Institut National Polytechnique de Toulouse (INPT), Toulouse, in 1978 and 1984, respectively.

From 1980 to 1988, he was a Researcher with the French National Center for Scientific Research, Laboratoire d'Electrotechnique et d'Electronique Industrielle. Since 1988, he is a Professor in Université de Lorraine, Nancy, France, and currently director of the Group of Research in Electrical Engineering of Nancy (GREEN). His research interests include power electronics, drives and new electrical devices (fuel cells and supercapacitors).

Phatiphat Thounthong (M'09–SM'13) was born in Phatthalung, Thailand, on December 29, 1974. He received the B.S. and M.E. degrees in electrical engineering from King Mongkut's Institute of Technology North Bangkok (KMITNB), Bangkok, Thailand, in 1996 and 2001, respectively, and the Ph.D. degree in electrical engineering from Institut National Polytechnique de Lorraine (INPL)-Université de Lorraine, Nancy-Lorraine, France, in 2005.

Currently, he is an Associate Professor in Department of Teacher Training in Electrical Engineering (TE), King Mongkut's University of Technology North Bangkok (KMUTNB). At present, he is the author of 72 scientific papers (including 16 papers in *IEEE Transactions/Magazines*) published in Scopus with *citations* = 1,317 times (without self-citations) and *h-index* = 17 (without self-citations). He is also the author and coauthor of four books entitled *Fuel Cell Energy Source for Electric Vehicle Applications* (New York: Nova Science, 2008; *Recent Advances in Supercapacitors* (Kerala: Transworld Research Network, 2006), *Progress in Fuel Cell Research* (New York: Nova Science, 2007), and *Polymer Electrolyte Membrane Fuel Cells and Electrocatalysts* (New York: Nova Science, 2009).

Dr. thounthong was the recipient of the *First Prize Paper Award* of the IEEE Industry Applications Society-Industrial Automation and Control Committee in 2009 (Texas-USA); the *Third Prize Oustanding Paper Award* of the IEEE International Telecommunications Energy Conference in 2015 (Osaka-Japan); the *Best Poster Presentation Award* of the IEEE International Conference on Electrical Machines in 2010 (Rome-Italy); and the *TRF-CHE-Scopus Researcher Awards* (Engineering & Multidisciplinary Technology) of the Thai Research Fund and Scopus Committee in 2012.

His current research interests include power electronics, electric drives, electric vehicles, electrical devices (Fuel cells, Photovoltaic, Wind turbine, Batteries, and Supercapacitors), non-linear controls and observers.